52nd AIAA/ASME/ASCE/AHS/ASC Structures, Structural Dynamics and Materials Conference
 19th
4 - 7 April 2011, Denver, Colorado

AIAA 2011-2079

Aeroelastic Analysis and Optimization at Conceptual Design Level Using NeoCASS Suite

L. Cavagna *, S. Ricci †and L. Travaglini ‡

The present work outlines NeoCASS, the Next Generation Computational Aero-Structural Sizing Suite, developed at the Department of Aerospace Engineering of Politecnico di Milano. The computational suite is completely developed within MATLAB© environment and aims at the structural sizing and aeroelastic analysis and optimization at the Aircraft Conceptual Design stage.

NeoCASS is part of a more complex multidisciplinary procedure able to completely tackle the conceptual design starting from a simple parametric geometry description and encompassing issues related to aerodynamics, flight performances, stability and control, propulsion and finally strucures/aeroelasticity. The whole design tool has been developed in the frame of SimSAC (Simulating Aircraft Stability And Control Characteristics for Use in Conceptual Design) project, funded by EU in the context of 6th framework Program (www.simsacdesign.eu).

The paper is mainly focused on the recent developments of NeoCASS, such as the modifications of Doublet Lattice Method to include in-plane effects and the implementation of the flutter constraint to be included in the multidisciplinary design optimization.

Introduction

The SimSAC project focused on enhancing the conceptual design and early preliminary design processes by developing an integrated environment; given any aircraft configuration, the aerodynamic response for stability and control assessment can now be computed at some user-defined fidelity level right from the conceptual design phase. Details about SimSAC and the complete software developed for the design process, called CEASIOM (Computerized Environment for Aircraft Synthesis and Integrated Optimization Methods), can be found in Ref.[1] Within the CEASIOM suite, the main goal of NeoCASS is to provide a realistic conceptual structural configuration, by coupling specifically developed structural models such as equivalent plates and linear/non-linear beams with low and high fidelity aerodynamic codes (Vortex and Doublet Lattice Methods, external CFD codes) to create a user-defined hierarchical set of tools for aeroelastic analysis and optimization with raising complexity and computational cost.

The estimation of the structural weight is an important part of the conceptual design of an airplane. It is necessary to know with considerably accuracy how much the airplane will weigh and the stiffness distribution precluding failures and satisfying strength, stiffness and, more generally speaking, aeroelastic constraints, e.g. stress, fatigue, buckling, flutter, control surface effectiveness, manufacturing and costs to mention a few. A large error in weight estimation will usually have far-reaching effects in the design. If such goal is not based on sound structural principles, the estimation will be likely to be unreasonable leading to serious difficulties. The classical approach based on the used of statistical formula is no more applicable for unconventional

*PostDoc Fellow, Dipartimento di Ingegneria Aerospaziale, Politecnico di Milano - Italy, Luca.Cavagna@polimi.it
†Associate Professor, Dipartimento di Ingegneria Aerospaziale, Politecnico di Milano - Italy, Sergio.Ricci@polimi.it.
‡Research Engineer, Dipartimento di Ingegneria Aerospaziale, Politecnico di Milano - Italy, Lorenzo.Travaglini@mail.polimi.it.

configurations and new technological concepts. For this reason, the first target of NeoCASS is to provide a more realistic prediction for the total structural weight, relying on physical basis rather than on the statistical/empirical methods commonly used.

A second important topic tackled is the capability to include stiffness and aeroelastic constraints starting from the conceptual design. The latter represents a key point since, generally speaking, all available procedures for conceptual design do not take into account aeroelastic requirements, postponing them to subsequent detailed design phases. Modern transport aircraft show nowadays high structural flexibility with full frequency overlapping between flight mechanics and structural dynamics. Thus, neglecting aeroelastic effects from the beginning could lead to the need of structural redesign resulting in weight and performance penalties. For this reason, the second top level target of NeoCASS suite is to include immediately in the design the capability to model the aeroelastic behavior, so that the user is provided with efficient tools for the aeroelastic analysis and optimization right from the beginning of conceptual design.
Since NeoCASS tool has been already described in previous papers (see for example [2,3,4]), in the following just a summary of the software capabilities will be reported. Much emphasis will be given to the latest developments and to few numerical applications.

I. NeoCASS Overview

NeoCASS is a suite of modules combining state of the art computational, analytical and semi-empirical methods to tackle all the aspects of the aero-structural analysis of a design layout at conceptual design stage. It gives a global understanding of the problem at hand without neglecting any aspect of it: weight estimation, initial structural sizing, aerodynamic performances, structural and aeroelastic analysis from low to high speed regimes, divergence, flutter analysis and determination of trimmed condition and stability derivatives both for the rigid and deformable aircraft.
As sketched in Figure 1, NeoCASS includes the following tools:

- Weight and Balance (WB) to have a prediction of non-structural masses and their location mainly based on statistical handbooks;
- GUESS (Generic Unknowns Estimator in Structural Sizing) to have a first guess analytical sizing of the airframe based on ultimate loads estimated on simple structural principles, linear aerodynamics and inertia distribution predicted by WB;
- SMARTCAD (Simplified Models for Aeroelasticity in Conceptual Aircraft Design) which is the numeric kernel for aero-structural analysis and optimization and can be used to enhance the solution provided by GUESS;
- MDO module, for the refinement of the initial structural sizing to meet specific aeroelastic constraints.

All the items share the same geometrical representation of the aircraft, fully described by a unique parametrization file based on the *Extensible Markup Language* (XML) format to which all different analysis modules refer. The geoemtry database is easily generated and managed in a visual environment by a dedicated module, named AcBuilder (see Figure 2). The adopted format allows storing each component of the aircraft and its parameter in a hierarchical and sorted way. It eases data sharing as well as the expansion of the dataset, i.e. the number of components of the aircraft can be modified at will by introducing new components as well as new parameters, thus increasing the family of morphologies that can be modeled. Besides the geometrical database, the XML format is also used by most modules included in CEASIOM, NeoCASS included, as a mean for specific data storing and transfer. This allows a high level of flexibility in updating and expanding each local database and guarantees, at the same time, a common format within the whole design framework.

As for the structural modelling, the *aircraft.xml* file also defines the structural concepts and material properties to adopted by GUESS during the initial structural sizing which leads to a first estimate of the

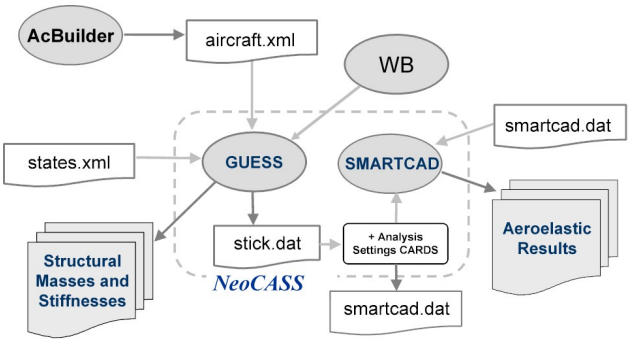

Figure 1. NeoCASS suite layout.

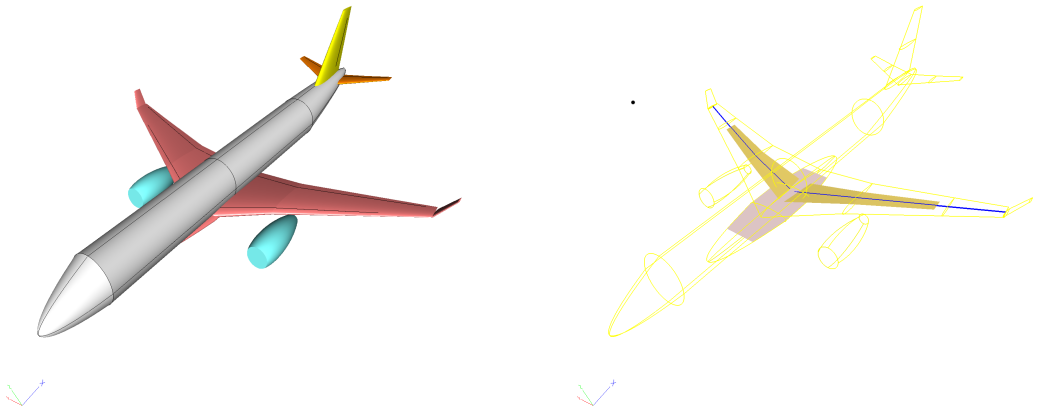

Figure 2. Aircraft representation using AcBuilder.

structural weight and stiffness distribution is available. A stick mesh model with all elements connectivity, material properties, non-structural lumped masses coming from WB can then be exported as a plain formated ASCII file *stick.dat*; this is the starting point in order to run the numeric aero-structural tool SMARTCAD. Further parameters are then provided as setting cards to the solver, so that each kind of analysis is correctly chosen and set. When these parameters are combined into the mesh file, a *smartcad.dat* file is available; the designer can at his will re-use and modify the input file to carry out the simulation required using SMARTCAD as a stand-alone application. Several outputs are finally available to the structural engineer for post-processing purposes, e.g. stresses, displacements and to the other modules in CEASIOM, e.g. stability derivatives, trimmed polars, vibration modes for flight-dynamic simulations including aeroelastic effects, under the hypothesis of small structural displacements. A Graphical User Interface (GUI) has been developed, allowing a user friendly access to all NeoCASS software modules, ranging from the preparation of the model, numeric analysis and post-processing of the results (see Figure 3).

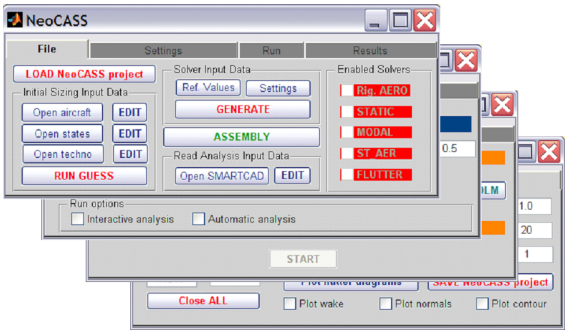

Figure 3. NeoCASS Graphical User Interface.

II. SMARTCAD for numeric aero-structural analysis and optimization

SmartCAD is the kernel dedicated to aeroelastic analysis and optimization. It allows the creation of low-order multi-fidelity models which can take into account most of the higher order/nonlinear effects and couplings for the aircraft to be designed, still keeping the total computational time limited. From the structural models point of view, SMARTCAD offers the choice between linear equivalent plates for low aspect ratio structures, linear beams for high aspect ratio structures and non-linear beams to include geometric effects when large displacements are involved. In particular, the beam used and showed here is based on a finite-volume formulation which does not require numerical integration but only the evaluation of equilibrium at collocation points and is free of shear-locking problems.[5] These models have a long tradition in the aerospace industry and are certainly important tools for preliminary structural analysis; these models are relative simple and require only few geometric details, hiding the real structural geometry up to the point of making the aircraft external shape partially or completely disappear. Despite the computational power available nowadays, these simplified models will be used for some time to come in aerospace industry, especially in the early design stage, where SMARTCAD is supposed to be adopted. They are indeed relatively accurate and allow to cheaply determine aeroelastic performances of the aircraft under design and to use the code within a MDO environment to drive aero-structural optimization into the proper direction. The code allows to carry out several kind of analysis such as: vibration modes, linearized flutter, linear[6] and non-linear[7] trim for the free-flying aircraft, aeroelastic corrections to stability derivatives.[8]

As for aerodynamic modelling, a hierarchic set of tools is available, according to the fidelity to be pursued:

- Vortex Lattice Method (VLM) for static aeroelasticity with camber contributions and deformable mesh

when non-linear beams are used to account for large displacements effects;

- Doublet Lattice Method (DLM)[9] to create Reduced Order Models (ROM) for unsteady generalized aerodynamic forces and rapidly discover flutter points at different Mach numbers in subsonic regime;
- Edge[10] CFD code to solve for Euler equations and predict flutter instabilities in the transonic regime, overcoming the unconservative flutter prediction (transonic dip) when linearized aerodynamic theories are used.[11]

The capabilities of NeoCASS suite and SMARTCAD module have been already presented; application cases of aeroelastic analysis and optimization in presence of buckling and static aeroelasticity constraints can be found in literature.[12,2]
The present paper is mainly focused on the implementation of the flutter constraint used during the structural optimization phase. As mentioned, SMARTCAD includes a dedicated tool for MDO. The optimization kernel is based on the MATLAB© optimization toolbox, implemented in a user friendly and flexible manner so that the user can set his specific optimization problem by defining at his will the objective and constraint functions. The design variables are usually represented by the stiffness distribution along wing span or section parameters like skin and web thickness and total bearing area. Polynomial expressions can also be introduced so to minimize the total number of design variables and result with a feasible solution. The optimization is finally solved following the typical approach based on the solution of a sequence of approximate explicit problems, obtained by linear and convex linear approximations of the considered aeroelastic responses, till convergence.

III. Enhanced DLM: in plane corrections

The Doublet Lattice Method (DLM) is one of the most common method for the evaluation of the unsteady aerodynamic loads. Nevertheless, some of the underlying assumptions turn out to be unsatifactory for some particular configurations. It is the case of T-empennages whose flutter point predictions are usually non-conservative. Experimental tests have indeed proved that most of the problems arise from the fact that:

1. unsteady aerodynamic loads are independent of the reference trim solution;
2. in-plane motion of aerodynamic surfaces are neglected in the definition of the loads;
3. aerodynamic loads are computed using the initial reference undeformed geometry.

When coupled to the reference steady solution (dependent on incidence and local deflections), the in-plane component of motion may give rise to considerable loads. The effect due to the deformed condition cannot be neglected as well.
These lacks have highligted for some configurations such as T-tails; the initial condition affects the unsteady loads computed by the linearized model, requiring correction terms to be included in order to improve the accuracy of the predictions. NeoCASS adopts the method presented in,[13] based on a combination of the two aerodynamic schemes (VLM and DLM) available in SMARTCAD.
The aerodynamic force on each panel can be computed by *Zhukovsky* relation:

$$\mathbf{f} = \rho\, \mathbf{v} \times \mathbf{\Gamma}\, l \tag{1}$$

where ρ, $\mathbf{v}$, $\mathbf{\Gamma}$ and l are respectively air density, velocity at the panel center point, vector of vortex intensity, and the spanwise length of the panel considered.

The velocity at the center point r_k (see Figure 4) is given by three contributions:

$$\mathbf{v}(r_k) = \mathbf{v}_\infty + \mathbf{v}^i(r_k, t) - \dot{\mathbf{u}}(r_k, t) \tag{2}$$

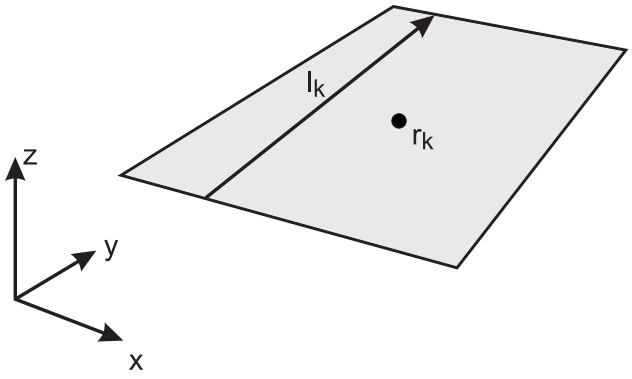

Figure 4. Aerodynamic panel

The terms at the right hand side are respectively the velocity of undisturbed flow, the velocity induced by the other panels and the effect due to the local motion. On each panel, the intensity $\mathbf{\Gamma}\, l$ can be written as:

$$\mathbf{\Gamma}\, l = \mathbf{l}_k \gamma_k \tag{3}$$

where $\mathbf{l}_k$ is the vector length of the panel and γ_k the vortex intensity.
Thus, the aerodynamic force on each panel k reads:

$$\mathbf{f}(r_k) = \mathbf{f}_k = \rho \left(\mathbf{v}_\infty + \mathbf{v}^i(r_k, t) - \dot{\mathbf{u}}(r_k, t) \right) \times \mathbf{l}_k \gamma_k \tag{4}$$

$\mathbf{l}_k$ is function of rotation $\boldsymbol{\varphi}(r_k, t)$ due to structural motion, in linearized form:

$$\mathbf{l}_k = \mathbf{l}_k^0 + \boldsymbol{\varphi}(r_k, t) \times \mathbf{l}_k^0 \tag{5}$$

The vortex intensity γ_k is given by the sum of the following three terms:

$$\gamma_k = \gamma_k^0 + \gamma_k^v(t) + \gamma_k^\varphi(t) \tag{6}$$

where:

- γ_k^0 comes from steady boundary conditions $(\mathbf{v}_\infty \cdot \mathbf{n}_k)$;
- γ_k^v comes from unsteady boundary conditions due to structural displacements $(\dot{\mathbf{u}}(r_k, t) \cdot \mathbf{n}_k)$;
- γ_k^φ comes from the unsteady boundary conditions due to structural rotations $(\mathbf{v}_\infty \cdot (\boldsymbol{\varphi}(r_k, t) \times \mathbf{n}_k))$.

Thus, the induced velocity is given by the sum of three terms:

$$\mathbf{v}^i(r_k, t) = \mathbf{v}^i(r_k)\gamma_k^0 + \mathbf{v}^i(r_k)\gamma_k^v(t) + \mathbf{v}^i(r_k)\gamma_k^\varphi(t) \tag{7}$$

Replacing Eq.(5), Eq.(6), Eq.(7) into Eq.(4), and considering first order terms only, the final expression for the aerodynamic force on each panel reads:

$$\mathbf{f}_k = \mathbf{f}_k^{00} + \mathbf{f}_k^{0v} + \mathbf{f}_k^{0\varphi} + \mathbf{f}_k^{v0} + \mathbf{f}_k^{\varphi 0} \tag{8}$$

where:

$$\mathbf{f}_k^{00} = \rho \left(\mathbf{v}_\infty + \sum_{j=1}^{N} \mathbf{v}_j^i(r_k)\gamma_j^0 \right) \times \mathbf{l}_k^0 \gamma_k^0$$

$$
\begin{aligned}
\mathbf{f}_k^{0v} &= \rho \left(\mathbf{v}_\infty + \sum_{j=1}^{N} \mathbf{v}_j^i(r_k)\gamma_j^0 \right) \times \mathbf{l}_k^0 \gamma_k^v(t) \\
\mathbf{f}_k^{0\varphi} &= \rho \left(\mathbf{v}_\infty + \sum_{j=1}^{N} \mathbf{v}_j^i(r_k)\gamma_j^0 \right) \times \mathbf{l}_k^0 \gamma_k^\varphi(t) \\
\mathbf{f}_k^{v0} &= \rho \left(\sum_{j=1}^{N} \mathbf{v}_j^i(r_k)\gamma_j^v(t) - \dot{\mathbf{u}}(r_k,t) \right) \times \mathbf{l}_k \gamma_k^0 \\
\mathbf{f}_k^{\varphi 0} &= \rho \left[\left(\sum_{j=1}^{N} \mathbf{v}_j^i(r_k)\gamma_j^\varphi(t) \right) \times \mathbf{l}_k^0 + \mathbf{v}_\infty \times \left(\boldsymbol{\varphi}(r_k,t) \times \mathbf{l}_k^0 \right) \right] \gamma_k^0
\end{aligned}
\tag{9}
$$

The term $\mathbf{f}_k^{00}$ is steady and is neglected for the evaluation of the stability of the system. Considering the unsteady contribution, the terms $\mathbf{f}_k^{0v}$ and $\mathbf{f}_k^{0\varphi}$ are those commonly computed by the DLM.
Finally, the terms $\mathbf{f}_k^{v0}$ and $\mathbf{f}_k^{\varphi 0}$ are the corrective terms coming from the steady solution (γ_k^0) and the induced velocities $\left(\sum_{j=1}^{N} \mathbf{v}_j^i(r_k)\gamma_j^v(t) \text{ e } \sum_{j=1}^{N} \mathbf{v}_j^i(r_k)\gamma_j^\varphi(t) \right)$ determined by the VLM.
Furthermore, to considerer the effects due to structural steady deformation, all terms are computed along the deformed reference condition. To validate the method outlined above, the testcase shown in Figure 5(a) has been considered. This is the same case reported in Ref.,[14] where experimental data are provided as well. The vertical tail is flexible and its deformability is represented by the first two natural modes (first bending and first torsional) only; the horizontal plane, on the other hand, is rigid. The flutter speed is then determined as function of the reference angle of attack α of the T-tail. Figure 5(b) shows the comparison between the numerical and experimental flutter points for $\alpha = 0$. As showed, the agreement is fairly good.

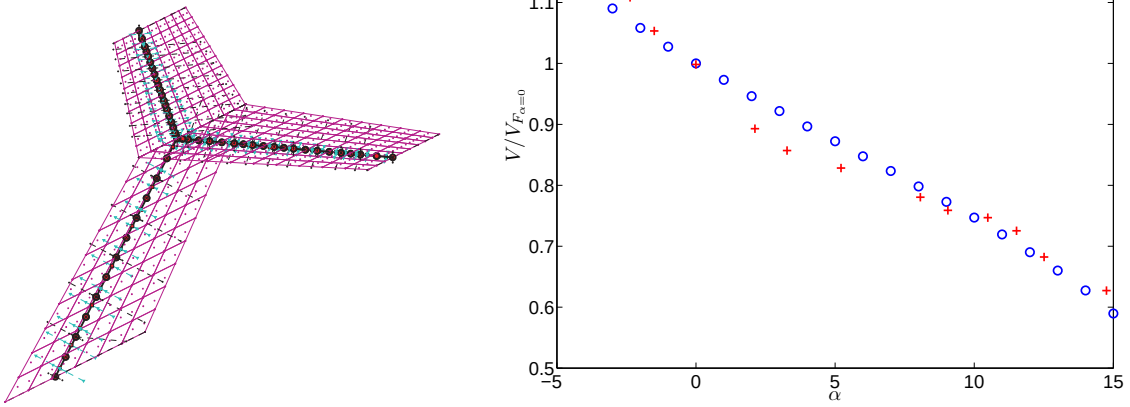

(a) T Empennage

(b) Flutter speed versus angle of attack

Figure 5. Validation Model

IV. Flutter Constraint Implementation

The flutter analysis technique implemented in SMARTCAD is based on a well consolidated continuation form. Adopting the classic assumptions based on assumed structural shapes, the availability of an aerodynamic transfer matrix $\mathbf{H}_{am}$ and the Laplace domain s, the flutter problem reads:

$$\left(s^2\,\mathbf{M} + s\,\mathbf{C} + \mathbf{K} - q_\infty \mathbf{H}_{am}(p, M_\infty)\right)\mathbf{q} \;=\; \mathbf{0} \tag{10}$$

where $\mathbf{q}$, $\mathbf{M}$, $\mathbf{C}$, $\mathbf{K}$ are respectively modal amplitudes, mass, damping, and stiffness matrices, and q_∞ is the dynamic pressure. Eq.(10) represents a complex eigenvalue problem in a non-canonic form, whose solution leads to flutter velocity, frequency and mode.

The method adopted here is the one proposed in,[15] where the Eq. 10 is solved as a nonlinear algebraic system of equations with the eigenvalue and the eigenvector as unknowns. The method is particularly suitable for optimization purposes since it unifies analysis and sensitivity calculation in a very effective way. The eigen-derivatives come from the solution of a linear system of equations that is determined trivially by differentiating the nonlinear equations with respect to a structural parameters. The coefficient matrix to be used is the same as the one used for the flutter-tracking process but with a different right hand side, keeping the computational cost very low and requiring only the knowledge of the eigenvectors and eigenvalues. See Ref.[16] for further details and Ref.[17] where an adjoint method is used to reduce the operations required for the calculation of the aeroelastic eigensensitivities, with a consequent substantial gain of efficiency, especially when a large number of parameters is involved in the design process.
The problem is non-linear and represented by n equation reported in Eq. (10) with n+1 unknowns represented by the n eigenvectors $\mathbf{q}$ and the eigenvalue s. A continuation method is adopted considering the velocity as a parameter and differentiating the system of equation to recover a system of differential equations. The eigensolutions are then determined within a range of flight velocities, usually from null up to a maximum given value. Given a velocity increment, few Newton-Raphson iterations are needed for the eigenproblem to converge. The solution is then used as starting point for the next velocity increment. Usually the process starts at null velocity considering as guess point the vacuum-vibration solution. Once the maximum velocity is reached, a new iterative tracking process is carried out starting from the next structural root. The mathematical expression of the problem is:

$$\left\{\begin{array}{c} \left(s^2\,\mathbf{M} + s\,\mathbf{C} + \mathbf{K} - q_\infty\,\mathbf{H}_{am}(p, M_\infty)\right)\mathbf{q} \;=\; \mathbf{0} \\ \frac{1}{2}\mathbf{q}^T\,\mathbf{q} - 1 = 0 \end{array}\right. = \left\{\begin{array}{c} \mathbf{F}(s,V)\,\mathbf{q} = \mathbf{0} \\ \mathbf{N}(\mathbf{q}) = 0 \end{array}\right. \tag{11}$$

where a normalization condition on eigenvectors is added to close and well-pose the problem. Its linearization leads to:

$$\left[\begin{array}{cc} \mathbf{F}(s,V) & \frac{\partial \mathbf{F}(s,V)}{\partial s}\,\mathbf{q} \\ \mathbf{q}^T & 0 \end{array}\right]\left\{\begin{array}{c} \Delta\mathbf{q} \\ \Delta s \end{array}\right\} = \left\{\begin{array}{c} -\mathbf{F}(s_0,V)\mathbf{q}_0 \\ 1 - \frac{1}{2}\mathbf{q}_0^T\,\mathbf{q}_0 \end{array}\right\} \tag{12}$$

Applying the continuation method:

$$\left\{\begin{array}{c} \frac{d}{dV}\left(\mathbf{F}(s,V)\,\mathbf{q}\right) = \mathbf{0} \\ \frac{d}{dV}\left(\mathbf{N}(\mathbf{q})\right) = 0 \end{array}\right. \tag{13}$$

results in a differential system with the same coefficient matrix as the linearized system given by Eq. (12):

$$\left[\begin{array}{cc} \mathbf{F}(s,V) & \frac{\partial \mathbf{F}(s,V)}{\partial s}\,\mathbf{q} \\ \mathbf{q}^T & 0 \end{array}\right]\left\{\begin{array}{c} \frac{d\mathbf{q}}{dV} \\ \frac{ds}{dV} \end{array}\right\} = \left\{\begin{array}{c} -\frac{\partial \mathbf{F}(s,V)}{\partial V}\mathbf{q} \\ 0 \end{array}\right\} \tag{14}$$

The previous system represents an initial value problem with initial solution equal to the structural solution for $V = 0$ which allows an efficient predictor-corrector technique to be applied. An explicit integration method is applied to Eq. (14) to have a first prediction which is then corrected by few Newton-Raphson

iterations given by Eq. (12). When converged, the eigenvalues sensitivities are recovered for free through Eq. (14). The same technique can be applied when direct flutter solution needs to be determined in terms of flutter speed and frequency.

The straightforward availability of eigenvalues derivatives with respect to the structural parameters makes this formulation well suited for the implementation of the flutter constraint. For a long time, the structural optimization able to include the flutter constraint has represented a challenge for aircraft designers. The approach based on the inclusion into the optimization problem of a specific constraint expressed in terms of flutter speed is generally affected by the presence of mode switching and hump modes, with continuous jumping inside and outside the feasible region during the optimization loop. For this reason, the choice adopted in many procedures presented in literature consists in to expressing the flutter constraint by means of a rejection curve applied to the so-called $V-g$ plot, i.e. aeroelastic damping g versus the flight speed V. The rejection curve is defined by the designer by assigning, for a preselected number of modes, a set of flight speed values for which a minimum value for the aeroelastic damping is required. In this way, one flutter constraint is transformed in N_d constraints corresponding to the selected velocity points. However, such implementation could be unpractical when using the flutter solution based on the continuation technique since the number of velocity points is not known a priori but defined run-time during the calculation on the basis of convergence criteria of the Newton-Raphson method. For this reason the flutter constraint in SMARTCAD is implemented as a single function for each mode followed during the mode tracking solution, obtained by combining in a boolean sense the area defined by the rejection curve and those defined by the modes affected by flutter (zero damping crossing points) or by hump modes. These area can be easily defined once the intersection points have been computed, as for example $1, 2, 3, 4$ in Figure 6. The goal of the optimization consists in minimizing the area given by the intersection of rejection area and those defined by the tracked modes, i.e. AREA1 and AREA2 in Figure 6.

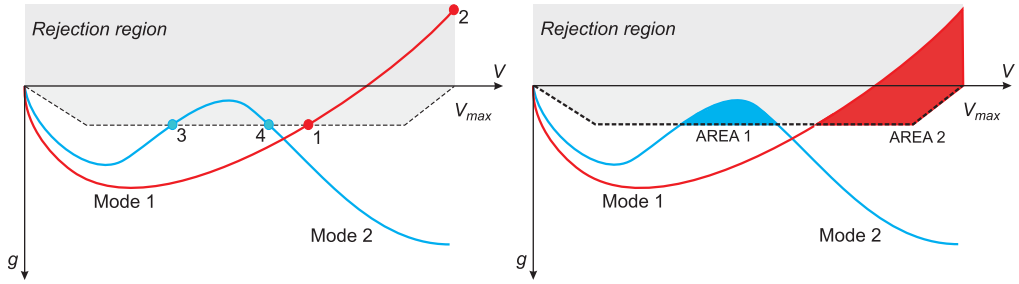

Figure 6. Implementation of the flutter constraint.

In general, for each mode i tracked, the total sum of the positive $g_d(V)$ area, normalized with respect to the total value recovered from its V-g plot, will be used as constraint during the optimization. In case the curve does not show any intersection with the rejection curve, the constraint is expressed as follows:

$$\text{CSTR} = \frac{\displaystyle\int_0^{V_{max}} g_d(V)dV}{0.5\displaystyle\int_0^{V_{max}} \left|g^0_{Vg}(V)\right| dV} \tag{15}$$

On the other hand, when intersections are present, the constraint is expressed as follows:

$$\text{CSTR} = \frac{\int_{z_1}^{z_2} g_d(V)dV + \int_{z_2}^{z_3} g_d(V)dV + \ldots + \int_{z_{n-1}}^{z_n} g_d(V)dV}{0.5\int_0^{V_{max}} \left|g^0_{Vg}(V)\right|} dV \tag{16}$$

where z_i represent the zeros of the $g_d(V)$ curve. The g^0_{Vg} area, computed at the first iteration, is used as normalization term and reported at the denominator.

For each mode shape subject to the flutter optimization, the process proceeds as:

1. identification of the mode inside the modal basis considered for the flutter problem;
2. calculation of the zeros of the function g_d;
3. calculation of the CSTR area ratio;
4. calculation of the derivatives of CSTR with respect to the design variables.

A well known difficulty in applying the flutter constraint is due to mode jumping, i.e. when the mode index showing the flutter changes during the iterations. Despite this could not appear as a major problem, provided that at the end of the optimization process all the considered modes do not show any crossing with the imposed rejection curve, the mode jumping could create convergence problems and in general oscillations of the solution trends, especially when gradient-based optimization algorithms are used as in this case. Thus, a mode identification process was introduced into the optimization based on a simple orthogonality check. Being $\mathbf{U}_{n-1}$ and $\mathbf{U}_n$ the modal bases corresponding to the iterations $n-1$ and n, respectively, the position of the i-th mode inside the modal base at the next iteration will be obtained by maximizing the following orthogonality scalar:

$$^i\mathbf{u}^T_{n-1} \cdot \mathbf{M}_n \cdot {}^j\mathbf{u}_n \tag{17}$$

where $\mathbf{M}_n$ is the global mass matrix at iteration n. In this way, a vector computed as following is saved

$$v(i) = j_{max} {}^i\mathbf{u}^T_{n-1} \cdot \mathbf{M}_n \cdot {}^j\mathbf{u}_n \tag{18}$$

which contains in the position i, for the considered mode, the actual position j of the same mode at the iteration n. Let's consider the following example, where the modal base of the generalized flutter problem is composed by the first 10 mode shapes [1 2 3 4 5 6 7 8 9 10] and the flutter constraint is applied to the mode 8 only. If at iteration n a mode switch happens between modes 7 and 8, the vector v resulting from the orthogonality check will appear as follows:

$$\begin{array}{lcccccccccc} (n-1) & 1 & 2 & 3 & 4 & 5 & 6 & 7 & \boxed{8} & 9 & 10 \\ & & & & & & & & \downarrow & & \\ v = & [1 & 2 & 3 & 4 & 5 & 6 & 8 & 7 & 9 & 10] \\ & & & & & & & & \swarrow & & \\ (n) & 1 & 2 & 3 & 4 & 5 & 6 & \boxed{7} & 8 & 9 & 10 \end{array} \tag{19}$$

During the next iteration the flutter constraint will be applied to the mode 7 in place of mode 8.

Finally, the derivatives of the flutter constraint are easily computed thanks to the continuation form adopted for the solution of the flutter problem. Indeed, by differentiation of the flutter problem with respect to the design variable p it is possible to write:

$$\begin{bmatrix} \mathbf{F}(s,V) & \dfrac{\partial\,\mathbf{F}(s,V)}{\partial\,s}\mathbf{q} \\ \mathbf{q}^T & 0 \end{bmatrix} \begin{Bmatrix} \dfrac{d\mathbf{q}}{dp} \\ \dfrac{ds}{dp} \end{Bmatrix} = \begin{Bmatrix} -\dfrac{\partial\mathbf{F}(s,V)}{\partial p}\mathbf{q} \\ 0 \end{Bmatrix} \tag{20}$$

The coefficients matrix has been already factorized and saved during the flutter analysis so that the derivatives calculation requires only the assembling of the right-hand term:

$$\frac{\partial\mathbf{F}(s,V)}{\partial p} = \left(s^2\frac{\partial\mathbf{M}}{\partial p} + s\frac{\partial\mathbf{C}}{\partial p} + \frac{\partial\mathbf{K}}{\partial p}\right) \tag{21}$$

During the iterations, for each design variable the derivatives of structural matrices are computed by finite difference then, once the flutter solution (s and $\mathbf{q}$) is available, the right-hand term is computed for each mode and for each speed value. Finally, the derivative of the entire $g_{Vg}(V)$ curve with respect to the design variable p will be:

$$g^p_{Vg}(V) = g_{Vg}(V) + \frac{\partial\,g_{Vg}(V)}{\partial p}dp \tag{22}$$

By applying the same procedure on the $g^p_{Vg}(V)$ curve to calculate the constraint value for a variation of the design variable p, i.e. CSTR^p, it is finally possible to calculate the derivative of flutter constraint by finite difference as follow:

$$\frac{\partial\,\mathrm{CSTR}}{\partial\,p} = \frac{\mathrm{CSTR}^p - \mathrm{CSTR}}{dp} \tag{23}$$

V. Numerical Example

Two different numerical examples will be discussed: in the first one NeoCASS suite is used to perform the conceptual design of a typical wide body, two engines, large aircraft. In the second one the flutter optimization of a regional twin-prop aircraft with a T-Tail configuration is reported.

V.A. Conceptual Design of a Two-engines Large Transport Aircraft

The main goal of this example is to demonstrate the versatility of NeoCASS suite in the conceptual aircraft design phase where it offers to the designer the change to quickly provide a complete aeroelastic model starting from a limited set of geometrical characteristics as well as the mission requirements. Indeed, the considered aircraft is based on the geometrical data of A350 available on the open literature, and for this reason is called A3XN. Figure 7 shows an overview of A3XN aircraft as described by AcBuilder tool.

NeoCASS offers two options for the structural sizing process within its module GUESS. For the first one (GUESS in standard mode), few pre-defined maneuvers based on the certification rules are adopted to derive the aircraft loads adopted for the structural sizing: specifically, a single pull-up maneuver at maximum load factor plus a sideslip maneuver due to an engine-off condition. For the second one (GUESS in modify mode) the user has the possibility to specify a set of maneuvers that are used to trim the rigid aircraft subject to aerodynamic loads computed by VLM method. It could be interesting for the designer to investigate the influence of different adopted maneuvers on the final structural weight of the aircraft. In the following a comparison among the sizing results obtained using the two options of GUESS module is reported. In particular, the set of sizing maneuvers adopted in Guess modify mode includes the following:

1. Normal load factor $n_z = 2.5$, $z = 0$ m, $M_\infty = 0.6$;

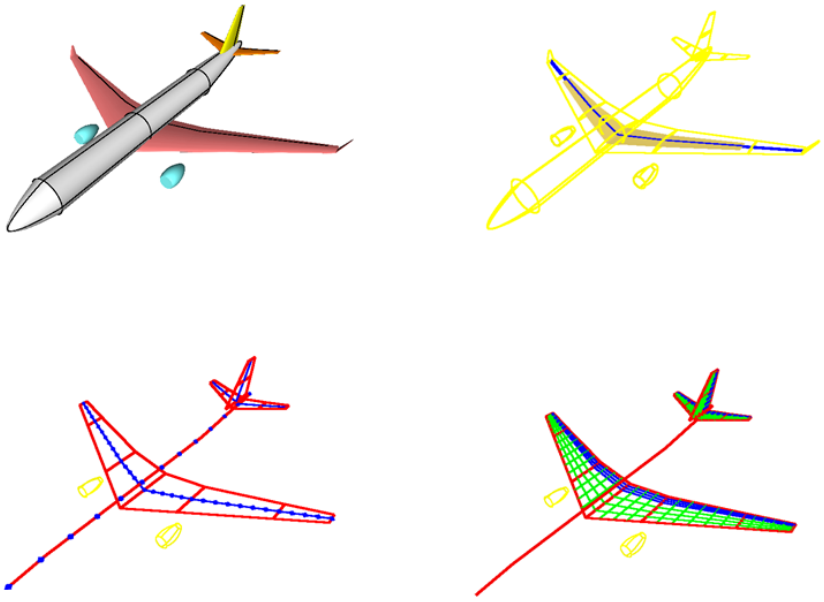

Figure 7. Overview of A3XN: external geometry, fuel, structural stick model and aerodynamic model.

2. Cruise flight with sideslip angle $\beta = 25$ deg, $z = 0$ m, $M_\infty = 0.65$;
3. A transition from levelled flight into a snap-roll given abrupt deflection on the elevator and the rudder, $z = 0$ m, $M_\infty = 0.6$, $\delta_e = 20$ deg, $\delta_r = 20$ deg.;
4. An abrupt roll maneuver with $\delta_a = 20$ at $z = 0$ m, $M_\infty = 0.6$.

Some examples of the typical output of a GUESS session are reported in Figures 8 and 9; the former shows the stick model generated by GUESS while the latter reports the internal loads due to the Load Condition N.1 used in modify mode.

Table 1 compares the final structural masses obtained using GUESS in standard and modify modes respectively. The results are simlar in the case of A3XN aircraft. It worths saying the aeroelastic stick model of the full aircraft is generated in few seconds or minutes, almost hands-off from the user point of view.

Component	**GUESS Standard** [kg]	**GUESS Modify** [kg]
Wing	19349	19883
Fuselage	15596	15043
Fin	946	829
Horizontal Tail	1515	1030

Table 1. Weight breakdown of A3XN obtained with GUESS in standard and modify mode.

Once available the aeroelastic stick model, it is possible to start a SMARTCAD run session where the typical static and dynamic aeroelastic responses are computed. For example, Table 2 shows the ratio of the

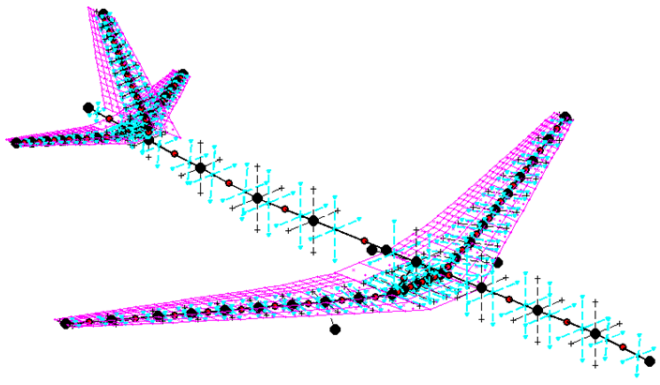

Figure 8. The stick model of the A3XN aircraft automatically generated by GUESS module.

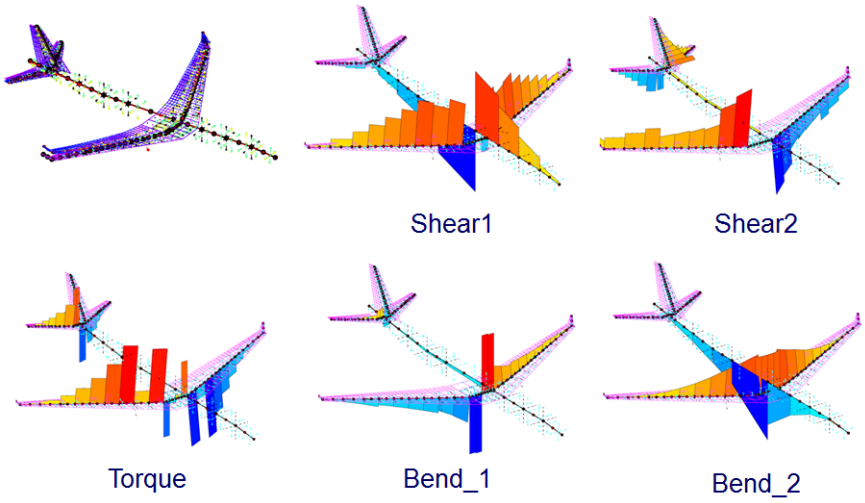

Figure 9. Internal loads of A3XN due to the Load Condition N.1.

relevant deformable over rigid stability and control derivatives, while Figure 10 shows the final V-g flutter results, in this case related to the aircraft configuration obtained using GUESS modify.

Derivative	GUESS Standard Deformable/Rigid	GUESS Modify Deformable/Rigid
C_{M_α}	0.87253	0.7618
$C_{L_{\delta_a}}$	0.52139	0.6270
$C_{M_{\delta_e}}$	0.71816	0.5790
$C_{N_{\delta_r}}$	0.63731	0.7970

Table 2. Comparison among the deformable vs. rigid values of relevant stability and control derivatives.

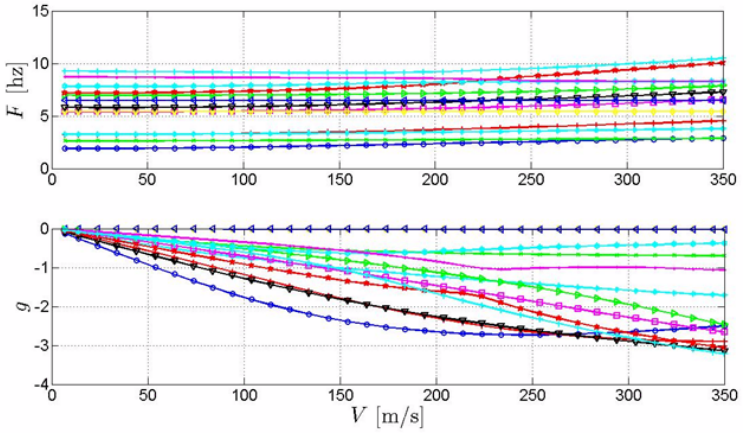

Figure 10. V-g plot of A3XN aircraft.

V.B. Twin-Prop Aircraft T-Tail Flutter Optimization

The considered example concerns a typical twin turboprop aircraft, with a MTOW equal to 27000 kg and a maximum numbers of passengers equal to 72. Figure 11 shows the aircraft geometry and the stick model defined using the AcBuilder tool. After the initial structural sizing obtained using GUESS module, the flutter analysis has been started using SMARTCAD. The flutter model is based on the first 20 vibration modes, including the first 6 rigid body modes. Nevertheless, only the modes involving the tail planes are considered during the tracking procedure. The aircraft shows a typical low speed flutter, involving horizontal and vertical tails. This is quite common for aircraft with a T-Tail configuration. Figure 12 shows the first 5 mode shapes involving the T-Tail participation. In particular, Modes 7 and 8 are those leading to the flutter mechanism.

The optimization process aims at increasing the flutter speed by working on the structural design variables initially defined by GUESS module. The optimization is mainly focused on the vertical tail, modeled using 4 beam elements. For each beam element the skin and web thicknesses and the distance among the section webs are considered as design variables, as shown in Figure 13. Thus, a total of 12 design variables defines the optimization problem, formulated as follows:

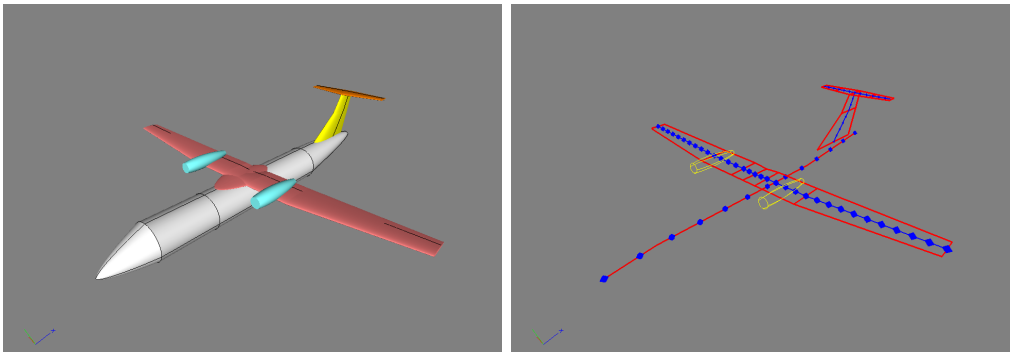

Figure 11. Twin turboprop aircraft representation using AcBuilder.

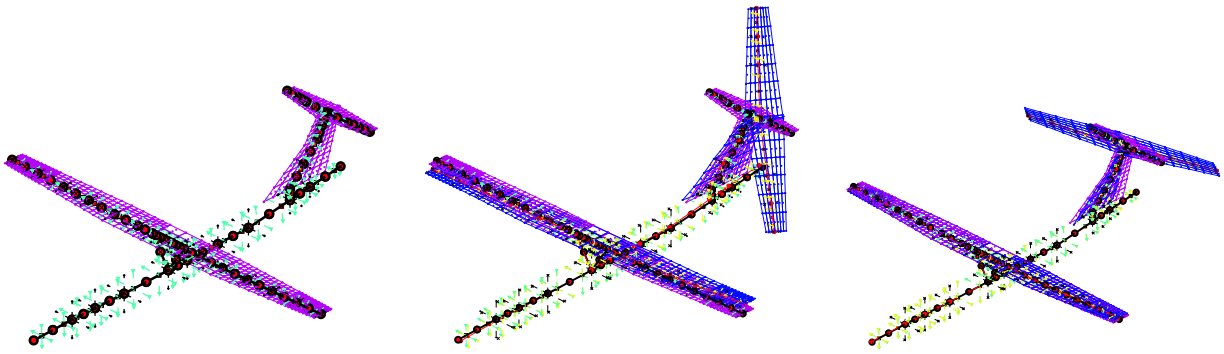

(a) Aeroelastic model (b) Mode 7 (c) Mode 8

(d) Mode 10 (e) Mode 11 (f) Mode 12

Figure 12. Twin-prop aeroelastic model and first 5 mode shapes

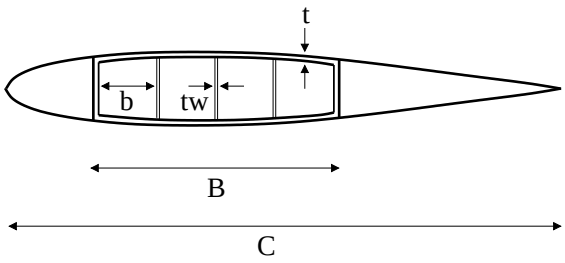

Figure 13. Design variables used during the MDO process.

$$\begin{array}{lll} \text{minimize :} & OBJ = \frac{W_{Opt}}{W_{Ini}}(d_j) & \\ \text{with respect to :} & d_j, & j = 1, \ldots, 12 \\ \text{subject to :} & CSTR(d_j) \geq 0, & \text{for Modes} = 7, 8, 10, 11 \; and \; 12 \end{array} \tag{24}$$

aiming at minimize the structural weight penalty ($\frac{W_{Opt}}{W_{Ini}}$) moving the V-g curves of first 5 mode shapes out of the requested rejection curve, so allowing for a flutter speed greater than 250 m/s. Figures 14 show the OBJ and flutter constraint trends during the iterations. Figure 15 compares the the initial and final properties of the vertical tail sections.

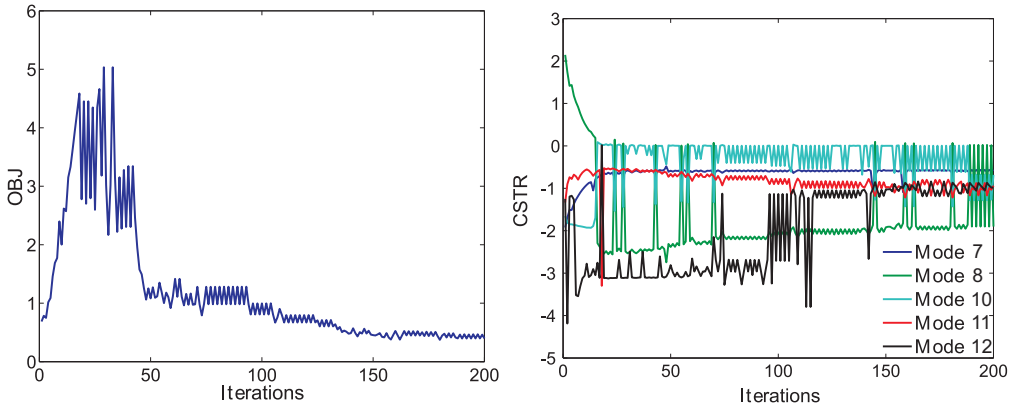

Figure 14. Histories of OBJ and flutter constraint during iterations.

Looking at the obtained results, it appears that the convergence is very poor, mainly due to the small move limits applied to the design variables (maximum design parameter variation of 10% allowed during each inner optimization loop) and to the convergence criterion (maximum OBJ variation less then $1.E-3$). Finally, Figure 16 shows the comparison between the initial and final V-g plots. Besides leading to a decrement of approximately 55% in the structural weight of the vertical tail, the optimization process increases the flutter speed from the initial value of 100 m/s to over 250 m/s. This result is obtained through a stiffness redistribution along the vertical tail structure, by a decrease in the stiffness close to the connection between the vertical tail and the fuselage, and at the same time by an increase of stiffness in correspondence of the vertical and horizontal tail connection.

The optimization results previously described have been obtained without the corrections to DLM described in Section III, so it could be interesting to investigate the effect of DLM corrections to the flutter

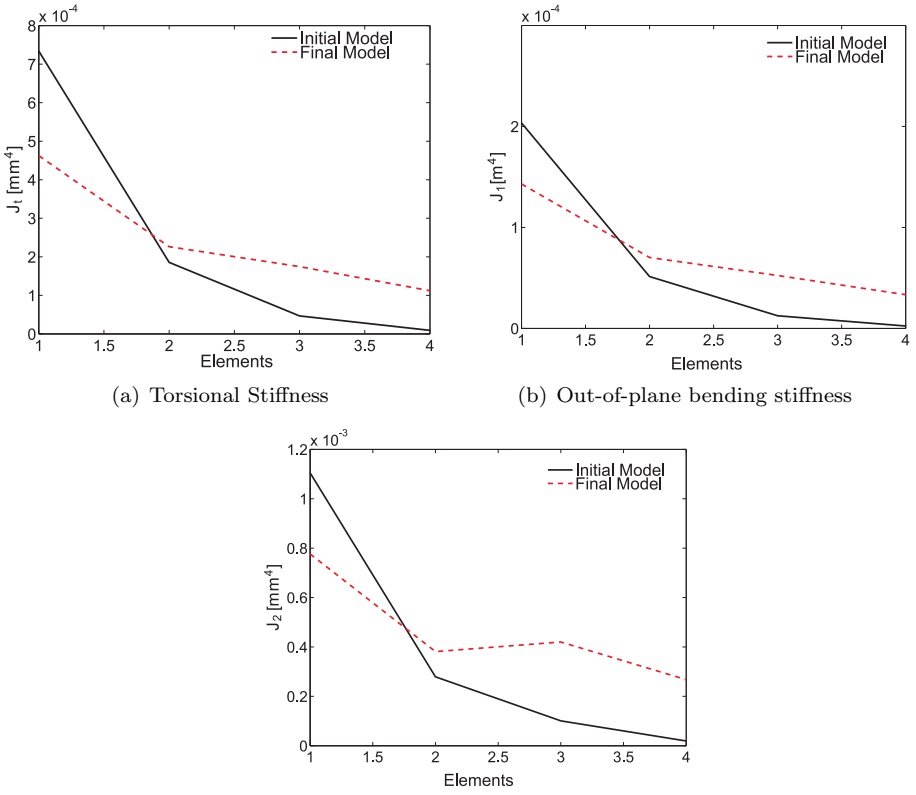

(a) Torsional Stiffness

(b) Out-of-plane bending stiffness

(c) In-plane bending stiffness

Figure 15. Comparison among initial and final structural properties of the vertical tail.

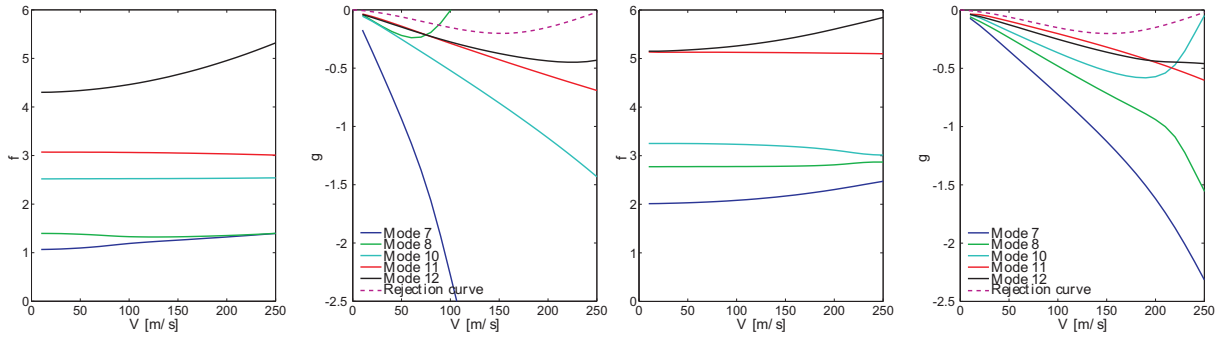

Figure 16. Initial and final Vg plot, without DLM corrections.

behavior of the optimized fin. It appears that the tenth mode shape, one involved in the flutter mechanism, is one mainly influenced by these corrections, with a change in both frequency and damping versus the flight speed. For this reason, a second optimization loop has been performed after introducing the DLM corrections. The convergence was obtained with very few iterations and not significant variation among the design variables. Figure 17 shows the comparison between the tenth mode V-g plot without and with DLM corrections, as well as the final V-g plot after the second optimization loop (in this last figure the flutter mode is labeled as Mode 3).

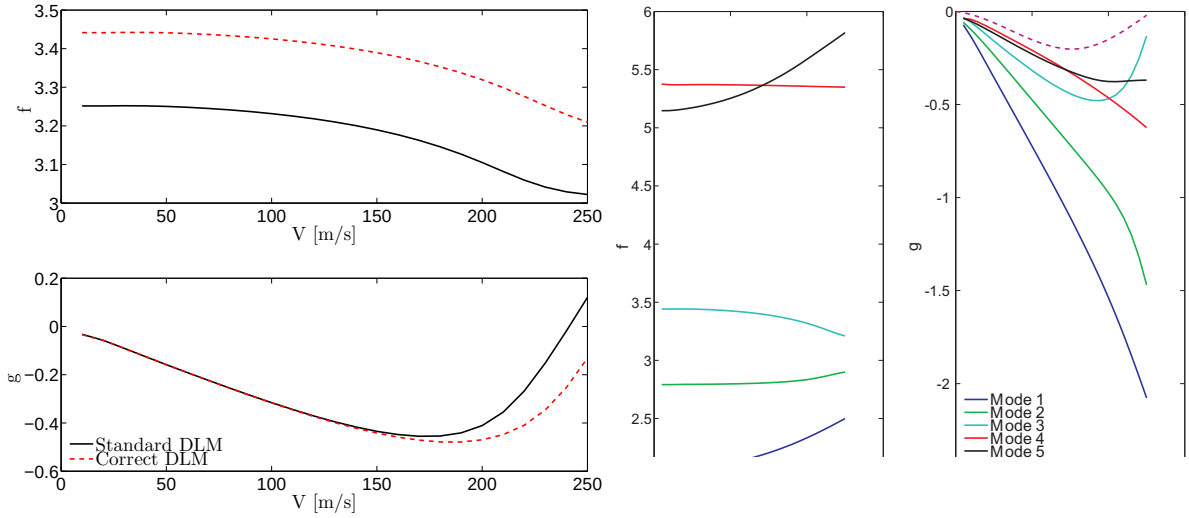

Figure 17. Influence of DLM corrections on flutter mode and the final VG plot after the second loop optimization.

Conclusions

This work summarizes the main features of a software environment for aero-structural conceptual design, named NeoCASS, which allows the fast design of the airframe once the geometrical configuration is defined. It is composed by different modules allowing the user to tackle all the aspects typical of aircraft conceptual design phase, starting from the initial weight and balance analysis, through the first structural sizing, till the final structural optimization. In particular the procedure includes a specific module, named SMARTCAD aiming at the aeroelastic analysis and optimization. The recent devolopments of SMARTCAD module include the corrections to DLM in case of relevant static or in-plane contributions like for T-Tail aircraft as well as a new implementation of the flutter constraint to be used during the MDO analysis. Two numerical examples are reported to demonstrate the validity of the proposed approach.

References

[1]Von Kaenel, R., Rizzi, A., Grabowski, T., andL. Cavagna, M. G., Ricci, S., and Bérard, A., "Bringing Adaptive-Fidelity CFD to Aircraft Conceptual Design: CEASIOM." *Proceedings of the* 26th *ICAS Congress*, Anchorage, Alaska, 14–19 September 2008.

[2]Cavagna, L., Ricci, S., and Riccobene, L., "A Fast Tool for Structural Sizing, Aeroelastic Analysis and Optimization in Aircraft Conceptual Design," *Proceedings of the* 50th *AIAA/ASME/ASCE/AHS/ASC Structures, Structural Dynamics and Materials Conference*, Palm Springs, CA, USA, 4–7 May 2009.

[3]Cavagna, L., Ricci, S., and Travaglini, L., "Structural Sizing and Aeroelastic Optimization in Aircraft Conceptual Design Using Neocass Suite," *Proceedings of the* 13th *AIAA/ISSMO Multidisciplinary Analysis and Optimization Conference*, Fort

Worth, Texas, USA, 13–15 September 2010.

[4]Cavagna, L., Ricci, S., and Travaglini, L., "NeoCASS: an Integrated Tool for Structural Sizing, Aeroelastic Analysis and MDO at Conceptual Design Level," *Proceedings of the 2010 AIAA/AIAA Atmospheric Flight Mechanics Conference*, Toronto, Canada, 2–5 August 2010.

[5]Ghiringhelli, G. L., Masarati, P., and Mantegazza, P., "A Multi-Body Implementation of Finite Volume Beams," *AIAA Journal*, Vol. 38, No. 1, January 2000, pp. 131–138.

[6]Rodden, W. and Love, J., "Equations of Motion of a Quasisteady Flight Vehicle Utilizing Restrained Static Aeroelastic Characteristics," *Journal of Aircraft*, Vol. 22, No. 3, 1985, pp. 802–809.

[7]Cavagna, L., Masarati, P., Ricci, S., and Mantegazza, P., "Development and Validation of an Investigation Tool for Nonlinear Aeroelastic Analysis," *Proceedings of the* 26^{th} *ICAS Congress*, Anchorage, Alaska, 14–19 September 2008.

[8]Rodden, W. and Gesling, J., "Application of oscillatory Aerodynamic theory to estimation of stability derivatives," *Journal of Aircraft*, Vol. 7, No. 3, 1970, pp. 272–275.

[9]Albano, E. and Rodden, W. P., "A Doublet–Lattice Method for Calculating the Lift Distributions on Oscillating Surfaces in Subsonic Flow," *AIAA Journal*, Vol. 7, No. 2, 1969, pp. 279–285.

[10]Eliasson, P., "A Navier-Stokes Solver for Unstructured Grids." FOI/FFA report FOI-R-0298-SE, FOI, 2001.

[11]Cavagna, L., Quaranta, G., and Mantegazza, P., "Application of Navier-Stokes simulations for aeroelastic assessment in transonic regime," *Computers & Structures*, Vol. 85, No. 11-14, 2007, pp. 818–832, Fourth MIT Conference on Computational Fluid and Solid Mechanics.

[12]Cavagna, L., Riccobene, L., Ricci, S., Berard, A., and Rizzi, A., "Fast MDO Tool for Aeroelastic Optimization in Aircraft Conceptual Design," *Proceedings of the* 12^{th} *AIAA/ISSMO Multidisciplinary Analysis and Optimization Conference*, Victoria, British Columbia, Canada, 10–12 September 2008.

[13]Chuban, V. D., "Influence of Angle of Attack and Stabilizer Deflection on T Empennage Flutter," *AIAA Journal Of Aircraft*, February 2005.

[14]McCue, R. G. D. J. and Drane, D. A., "The Effects of Steady Tailplane Lift on the Subcritical Response of a Subsonic T-Tail Flutter Model," *Aeronautical Research Council Reports and Memoranda*, , No. 3652, 1971.

[15]Cardani, C. and Mantegazza, P., "Continuation and Direct Solution of the Flutter Equation," *Computers & Structures*, Vol. 8, 1978, pp. 185–192.

[16]Cardani, C. and Mantegazza, P., "Calculation of Eigenvalue and Eigenvector Derivatives for Algebraic Flutter and Divergence Eigenproblems," *AIAA Journal*, Vol. 17, No. 4, 1979, pp. 408–412.

[17]Bindolino, G. and Mantegazza, P., "Aeroelastic Derivatives as a Sensitivity Analysis of Nonlinear Equation," *AIAA Journal*, Vol. 25, No. 8, August 1987, pp. 1145–1146.